

# Rarefied Transitional Bridging of Blunt Body Aerodynamics

R. G. Wilmoth, R. C. Blanchard, J. N. Moss  
NASA Langley Research Center, Hampton, VA, USA

## 1 Introduction

Bridging relations are frequently used to provide engineering aerodynamic predictions in the transitional regime between free-molecular and continuum flows. Such predictions are important for mission studies of high-speed planetary entry vehicles to provide accurate analysis of trajectory dynamics, vehicle stability, and landing footprint. However, empirical parameters in these bridging relations must be derived from available experimental, flight, and computational data, where the latter is often generated using Direct Simulation Monte Carlo (DSMC) methods. Therefore, bridging relations have been sought that are applicable to a wide range of vehicles over a wide range of conditions and use a minimum number of empirical parameters [1, 2]. In the absence of a “universal” bridging relation, it is desirable to reduce the experimental and computational effort required to “calibrate” the bridging function for a particular class of vehicles.

The increase in planetary entry and Earth sample return missions in recent years has increased the need for rarefied transitional flow analysis. Mission studies have revealed a number of instances where transitional aerodynamics plays a significant role in trajectory and attitude control design, and DSMC analyses have been performed to investigate these issues [3, 4, 5]. These analyses have produced a rather extensive database of transitional aerodynamics for spherically-blunted cone geometries, and therefore it is appropriate to use this information to develop improved bridging relations for this class of vehicles. Furthermore, the good agreement recently shown between DSMC analyses and flight data [6, 7] provides increased confidence in the accuracy of the DSMC predictions.

The analysis in this paper uses rarefied aerodynamic predictions (Knudsen number,  $Kn_\infty \geq 0.001$ ) for Viking, Pathfinder, Microprobe, Mars’01 Orbiter, and Stardust vehicles under the nominal entry conditions shown in Fig. 1. These vehicles have spherically-blunted cone forebodies with conic or biconic afterbodies. Viking, Pathfinder, and Mars’01 Orbiter have 70-deg

half-angle cone forebodies, while Stardust and Microprobe have forebody cone half-angles of 60 and 45 deg, respectively. These missions are designed for direct entry at nominal velocities ranging from 4.5 to 12.6 km/s except for Mars'01 Orbiter which currently plans to perform an aerocapture trajectory entering the Mars atmosphere at about 6.6 km/s and exiting at about 3.5 km/s. All flights are Mars missions except Stardust which is a comet sample return to Earth. Viking results are of particular interest because flight data are available for comparison.

Several bridging approaches were explored, and a standard *sine-squared* relation [8] and an *erf-log* relation [7] were chosen to describe the variations in aerodynamic quantities from the free-molecular to the continuum regime. The purpose of this paper is to show the accuracy to which these relations describe the transitional aerodynamics for this particular class of blunt-body flows and to provide a nominal set of empirical parameters for use in engineering predictions of blunt-body aerodynamics.

## 2 Transitional Bridging Relations

Transitional bridging methods generally fall into the class of either “local” or “global” techniques. The functional relation used by both methods can be expressed in the form

$$C = P_b \cdot C_{fm} + (1 - P_b) \cdot C_{cont} \quad (1)$$

where  $C$  is a local (pressure, friction, etc.) or global (drag, lift, etc.) coefficient, and the subscripts  $fm$  and  $cont$  refer to the value of the coefficient in the free-molecular and continuum limits, respectively.  $P_b$  in Eq. (1) is the bridging function that defines the variation in the coefficient between the free-molecular and continuum limits using Knudsen number, Mach number, Reynolds number, or various combinations as independent variables.

A commonly used global bridging function is the *sine-squared* relation

$$P_b = \sin^2 \phi \quad (2)$$

where

$$\phi = \pi \cdot (a_1 + a_2 \log_{10} Kn_\infty) \quad (3)$$

and  $a_1$  and  $a_2$  are constants related to the Knudsen numbers,  $Kn_{fm}$  and  $Kn_{cont}$  that define the free-molecular and continuum limits. Eqs. (2)-(3) have been used for many of the planetary vehicles covered in this paper. However, deficiencies in this bridging relation were noted based on Shuttle flight data [8]. Also, the function is intended to be applied only within the limits  $0 \leq \phi \leq \frac{\pi}{2}$ .

The bridging function

$$P_b = \frac{1}{2} \left( 1 + \operatorname{erf} \left\{ \frac{\sqrt{\pi}}{\Delta Kn} \log \left[ \frac{Kn_\infty}{Kn_m} \right] \right\} \right) \quad (4)$$

was used by Ivanov [7] to describe Soyuz aerodynamics. In Eq. (4),  $Kn_m$  is the center of the transitional regime defined at  $P_b = \frac{1}{2}$  and  $\Delta Kn$  is the logarithmic width of the transitional regime. This relation, which Ivanov refers to as *erf* -  $\log Kn$  bridging, was applied in [7] as a local bridging relation but is applied in this paper as a global bridging relation.

### 3 Computational Approach

Axisymmetric and full three-dimensional free-molecular, DSMC, and continuum methods were used to compute the flowfields and aerodynamics for all vehicles. Axisymmetric DSMC calculations were performed using the G2 code of Bird [9] while three-dimensional free-molecular, DSMC and Newtonian calculations were performed using the DSMC Analysis Code (DAC) of LeBeau [10] and companion free-molecular/Newtonian codes described in [11]. A small number of Navier-Stokes results are included to complement the Newtonian predictions in the continuum limit.

Computations were performed for each vehicle over a range of flight conditions and attitudes that correspond to a nominal trajectory for the mission. Detailed flow conditions for the various trajectories are given in [3, 4, 5, 6].

## 4 Results

### 4.1 Viking Flight Comparisons

DSMC predictions of the ratio of normal-to-axial force are shown in Fig. 2 for the Viking 1 lander. Included are the measured flight data and results for both *sine-squared* and *erf-log* bridging relations. The overall agreement between flight data, DSMC predictions and bridging relations is excellent. However, the sensitivity of the accelerometers used for the flight measurements was not designed for the small forces experienced at the higher Knudsen numbers, and the flight data exhibit considerable scatter at these Knudsen numbers [12]. The *erf-log* function is evaluated outside the free-molecular and continuum limits imposed on the *sine-squared* function to illustrate the asymptotic behavior of the *erf-log* function.

### 4.2 Bridging Function Correlations

Drag predictions are shown in Fig. 3 for zero angle of attack,  $\alpha$ , for all except the Viking data which correspond to the nominal  $\alpha = 11 \text{ deg}$  achieved

during Mars entry. The data demonstrate the typical behavior of vehicles in transitional flow, and the drag variations are very similar. Notable exceptions occur near the free-molecular limit where the low-velocity Mars'01 exit trajectory yields higher drag coefficients than the other vehicles and at the continuum limit where the drag coefficients are lower for the smaller cone-angle vehicles. Additional small differences in vehicle drag are caused by differences in trajectory flight conditions.

Although the complete set of aerodynamic predictions is too extensive to include here, results were also computed at various angles of attack,  $\alpha$ , to yield an aerodynamic database for use in mission studies. The most complete set of calculations available are for the various 70-deg bodies (Viking, Pathfinder, and Mars'01 Orbiter). A subset of these results was selected for detailed correlations with both bridging functions. The functions were fit in a least-squares sense to DSMC predictions of the aerodynamic coefficients, and the “best-fit” parameters for Eqs. (2) and (4) were determined. The root-mean-squared (RMS) error for each function was calculated as an overall measure of the “goodness” of fit.

Typical bridging parameters for various aerodynamic coefficients for the Mars'01 case are given in Table 1. In general, the two bridging relations give about the same accuracy in axial and drag forces while the *erf-log* relation gives a somewhat better fit to other aerodynamic coefficients.

### 4.3 Single-Point Bridging Procedure

The bridging parameters given in Table 1 for  $\alpha = 11^\circ$  are typical of those obtained for other angles of incidence and vehicles. The parameters for each bridging function vary significantly for the various vehicle attitudes and shapes. However, the *erf-log* method has an advantage over the *sine-squared* method in that it is sensitive mainly to only one parameter,  $Kn_m$ , while the *sine-squared* method has about the same sensitivity to both parameters,  $a_1$  and  $a_2$ . Therefore, a procedure can be constructed for the *erf-log* method wherein a value for  $\Delta Kn$  is assumed, and the second parameter,  $Kn_m$ , is obtained from a single value of the coefficient at some intermediate Knudsen number in the transitional region. Such a procedure is illustrated in Fig. 4. By computing the aerodynamic coefficient,  $C$ , at the free-molecular and continuum limits and at some intermediate value of  $Kn_\infty$ , the bridging function value,  $P_b$ , is obtained. Given  $P_b$  and further assuming a “universal” value for  $\Delta Kn$  in Eq. (4), the second parameter,  $Kn_m$ , can be extracted.

Based on analysis of all the blunt-body DSMC results available, a value for  $\Delta Kn$  of  $\log 500 = 6.2146$  was chosen. The single-point bridging procedure was applied to the data where  $Kn_m$  was evaluated based on a single DSMC result that typically fell in the range  $0.05 \leq Kn_\infty \leq 0.5$ . A comparison of the bridging function thus obtained is shown in Fig. 5 for the Mars'01 data at

$\alpha = 11 \text{ deg}$ . The “goodness” of fit as determined by the RMS error was not significantly degraded by this procedure, and although the “universal” value of  $\Delta Kn$  was chosen mainly based on the Mars’01 predictions, this value applies reasonably well to the other vehicles. Table 2 shows the bridging parameters and RMS errors for axial force coefficient for all the data sets available, and the errors are generally less than 5 percent.

## 5 Concluding Remarks

The bridging procedures discussed provide an accurate engineering method for predicting rarefied transitional aerodynamics of spherically-blunted cone entry vehicles. The single-point procedure offers a way to improve the bridging procedures while minimizing the computational effort. However, the accuracy of these procedures ultimately depends on accurate knowledge of the aerodynamics in the free-molecular and continuum limits. The excellent agreement shown for DSMC predictions and bridging relations with the Viking flight data in transitional regime enhance the confidence in these procedures.

## References

- [1] Kotov, V. M., Lychkin, E. N., Reshetin, A. J. and Schelkonogov, A. N., *An Approximate Method of Aerodynamics Calculation of Complex Shape Bodies in a Transition Region, Rarefied Gas Dynamics*, Vol. 1, ed. O. M. Belotserkovskii, Plenum Press, 1985.
- [2] Potter, J. L, and Peterson, S. W., *Local and Overall Aerodynamics Coefficients for Bodies in Hypersonic Rarefied Flow*, AIAA Paper 91-0336, Jan. 1991.
- [3] Moss, J. N., Wilmoth, R. G., and Price, J. M., *DSMC Simulations of Blunt Body Flows for Mars Entries: Mars Pathfinder and Mars Microprobe Capsules*, AIAA Paper 97-2508, June 1997.
- [4] Moss, J. N., Blanchard, R. C., Wilmoth, R. G., and Braun, R. D., *Mars Pathfinder Rarefied Aerodynamics: Computations and Measurements*, AIAA Paper 98-0298, Jan. 1998.
- [5] Wilmoth, R. G., Mitcheltree, R. A., and Moss, J. N., *Low-Density Aerodynamics of the Stardust Sample Return Capsule*, AIAA Paper 97-2510, June 1997.
- [6] Blanchard, R. C., Wilmoth, R. G., and Moss, J. N., *Aerodynamic Flight Measurements and Rarefied-Flow Simulations of Mars Entry Vehicles*, J. of Spacecraft and Rockets, Vol. 34, No. 5, 1997, pp. 687-690.

- [7] Ivanov, M. S., Markelov, G. N., Gimelshein, S. F., Mishina, L. V., Krylov, A. N., and Grechko, N. V., *High-Altitude Capsule Aerodynamics with Real Gas Effects*, J. of Spacecraft and Rockets, Vol. 35, No. 1, 1998, pp. 16-22.
- [8] Blanchard, R. C., and Buck, G. M., *Rarefied-Flow Aerodynamics and Thermosphere Structure from Shuttle Flight Measurements*, J. of Spacecraft, Vol. 23, No. 1, 1986, pp. 18-24.
- [9] Bird, G. A., *The G2/A3 Program Users Manual*, G.A.B. Consulting Pty Ltd, Killara, N.S.W., Australia, Mar. 1992.
- [10] LeBeau, G. J., *A Parallel Implementation of the Direct Simulation Monte Carlo Method*, to be published in Computer Methods in Applied Mechanics and Engineering, 1998.
- [11] Wilmoth, R. G., LeBeau, G. J., and Carlson, A. B., *DSMC Grid Methodologies for Computing Low-Density Hypersonic Flows About Reusable Launch Vehicles*, AIAA Paper 96-1812, June 1996.
- [12] Blanchard, R. C., and Walberg, G. D., *Determination of the Hypersonic-Continuum/Rarefied-Flow Drag Coefficient of the Viking Lander Capsule I Aeroshell from Flight Data*, NASA TP 1793, Dec. 1980.

Coefficient	<i>sine-squared</i> Parameters			<i>erf-log</i> Parameters		
	$a_1$	$a_2$	RMS Error, %	$\Delta Kn$	$Kn_m$	RMS Error, %
$C_A$	0.2836	0.1000	3.9	6.5	0.3576	4.1
$C_N$	0.3107	0.0926	17.3	6.3	0.1804	7.0
$C_m$	0.3367	0.0921	19.8	5.9	0.0825	12.1

Table 1: Bridging relation parameters for various Mars'01 aerodynamic coefficients. Angle of attack = 11 deg.

Vehicle	$\Delta Kn$	$Kn_m$	RMS Error, %
Viking	6.2146	0.1805	4.3
Pathfinder	6.2146	0.1804	4.6
Mars'01	6.2146	0.4894	4.8
Stardust	6.2146	0.0756	4.8
Microprobe	6.2146	0.0475	5.8

Table 2: *erf-log* Bridging parameters for  $C_A$  for various vehicles using single DSMC point to determine  $Kn_m$ .

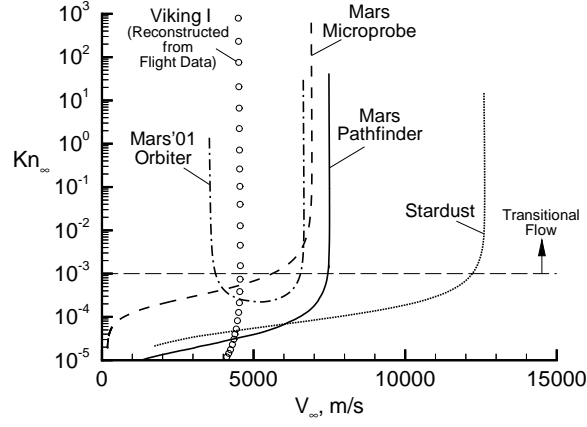


Figure 1: Nominal planetary entry trajectories.

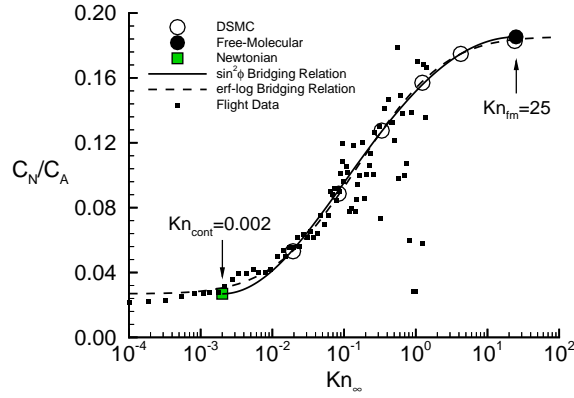


Figure 2: DSMC predictions and bridging relations compared to Viking I flight data. Ratio of normal-to-axial force coefficient,  $C_N/C_A$ .

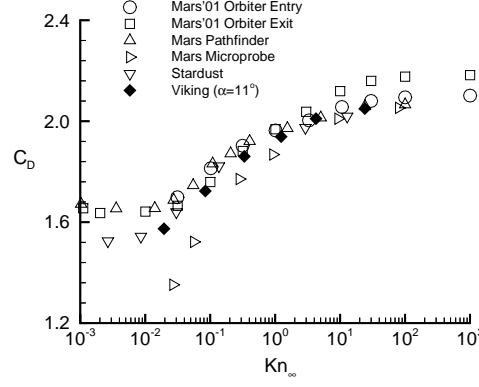


Figure 3: Drag predictions for various blunt bodies. Zero incidence for all except Viking for which  $\alpha = 11^\circ$ .

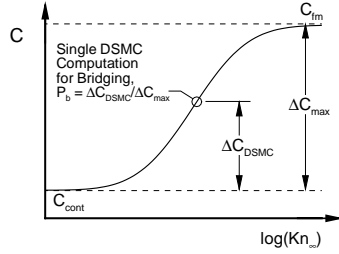


Figure 4: Procedure to determine bridging constant using single DSMC computation.

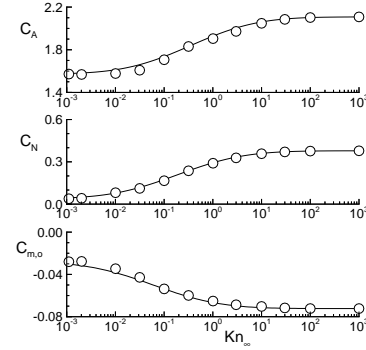


Figure 5: Aerodynamics for Mars'01 Orbiter from DSMC and *erf-log* bridging relation based on single-point fit. Symbols are DSMC, line is bridging relation.  $\alpha = 11^\circ$ .